NSTX

Supported by

U.S. DEPARTMENT OF ENERGY | Office of Science

Validation of RWM Kinetic Stability Model and Physics Implications in NSTX

J. Bialek, J.W. Berkery, S.A. Sabbagh

Department of Applied Physics, Columbia University, New York, NY, USA

R. Betti, R.E. Bell, A. Diallo, S.P. Gerhardt,

B.P. LeBlanc, J. Manickam, and M. Podestà

Princeton Plasma Physics Laboratory, Princeton, NJ, USA

Y.Q. Liu, I.T. Chapman

Euratom/CCFE Fusion Association, Culham Science Centre, Abingdon, OX14 3DB, UK

J.P. Graves

Ecole Polytechnique Federale de Lausanne (EPFL), Centre de Recherches en Physique des Plasmas, Association EURATOM-Confederation Suisse, 1015 Lausanne, Switzerland

Z.R. Wang

Consorzio RFX, Associazione EURATOM-ENEA sulla Fusione Corso Stati Uniti 4, 35127 Padova, Italy

53rd Annual Meeting of the Division of Plasma Physics

Salt Lake City, Utah November 16, 2011

Abstract

The resistive wall mode (RWM) instability may limit the promise of disruption-free operation in future tokamaks unless a reliable stabilization mechanism is found. Kinetic effects in the plasma can passively stabilize the mode by dissipating its energy. The change in potential energy by kinetic effects is calculated for experimental plasma equilibria with the MISK code. Further improvements of the theoretical model are presently being investigated to refine the quantitative agreement between computed RWM marginal stability points and experimental results. These include the role of collisions in both dissipating the mode energy and also in damping the resonant kinetic effects, and the inclusion of anisotropy of neutral beam injected energetic ions to correctly account for their stabilizing effects on RWM stability. Recent experiments in NSTX with reduced plasma internal inductance plasmas that have decreased RWM stability are consistent with MISK calculations. These kinetic stability calculations are being benchmarked through comparison with the results of other codes such as MARS-K and HAGIS. The implications of this physics for the stability of future devices, such as ITER, are also discussed. Supported by U.S. D.O.E. contracts DE-FG02-99ER54524, DE-AC02-09CH11466, and DE-FG02-93ER54215.

Resistive wall mode stability can be explained by including kinetic effects ; Code calculations require benchmarking

- Motivation
  - Accurate calculation of the physics of RWM kinetic stabilization is key for disruption-free operation of a low collisionality burning plasma (ST-CTF, FNSF, ITER) at any rotation.
- Outline
  - Recent resonant field amplification and reduced internal inductance experimental results in NSTX are consistent with kinetic stability theory as calculated by the MISK code.
  - Kinetic stability calculations are being benchmarked through comparison with the results of other codes such as MARS-K and HAGIS. (ITPA MHD Stability group joint experiment MDC-2)
  - Corrected stability calculations improve agreement with experiments in cases tested to date.

Kinetic terms in the RWM dispersion relation enable stabilization; theory consistent with experimental results

Dissipation (Im(δW_K)) and restoring force (Re(δW_K)) from kinetic term enables stabilization of the RWM:

$$(\gamma - i\omega_r)\,\tau_w = -\frac{\delta W_\infty + \delta W_K}{\delta W_b + \delta W_K}$$

[B. Hu *et al.*, Phys. Plasmas **12**, 057301 (2005)]

$$\delta W_K = \sum_j \sum_{l=-\infty}^{\infty} 2\sqrt{2}\pi^2 \int\!\!\int\!\!\int \left[|\langle H/\hat{\varepsilon}\rangle|^2 \frac{(\omega - n\omega_E)\frac{\partial f_j}{\partial \varepsilon} - \frac{n}{Z_j e}\frac{\partial f_j}{\partial \Psi}}{n\langle\omega_D^j\rangle + l\omega_b^j - i\nu_{\text{eff}}^j + n\omega_E - \omega} \right] \frac{\hat{\tau}}{m_j^{\frac{3}{2}} B} |\chi| \hat{\varepsilon}^{\frac{5}{2}} d\hat{\varepsilon}\, d\chi\, d\mathbf{\Psi}, \qquad \chi = v_\parallel / v$$

Precession Drift — Bounce — Collisionality — ~ Plasma Rotation: $\omega_\phi \approx \omega_E + \omega_{*i}$

$\gamma\tau_w$ contours vs. ν and ω_ϕ

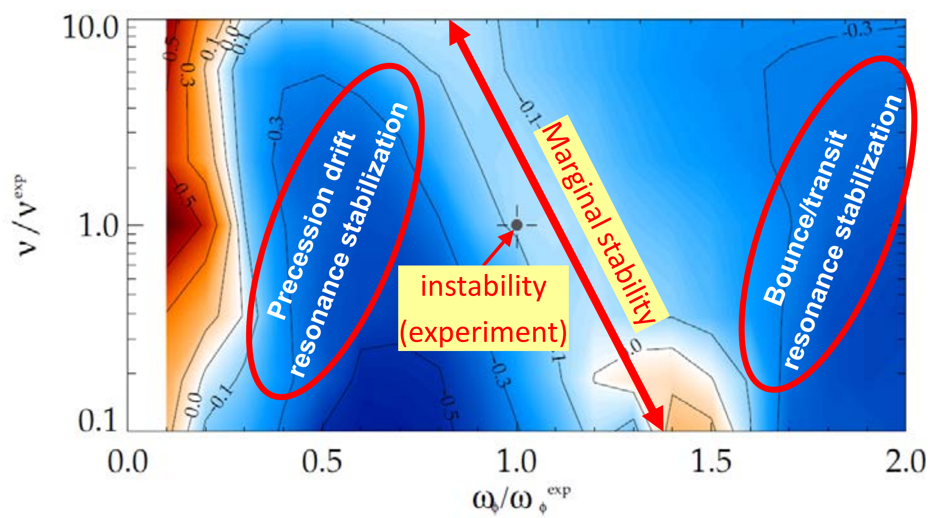

- MISK calculations are consistent with RWM instability at intermediate plasma rotation in NSTX
- Instability appears between precession drift resonance at low ω_ϕ, bounce/transit resonance at high ω_ϕ

[S. Sabbagh *et al.*, Nucl. Fusion **50**, 025020 (2010)]

[J. Berkery *et al.*, Phys. Rev. Lett. **104**, 035003 (2010)]

Improving quantitative agreement: EPs are generally stabilizing; Anisotropic distribution impacts stability

$$\delta W_K \sim \left[\frac{1}{\langle \omega_D \rangle + l\omega_b - i\nu_{\rm eff} + \omega_E} \right]$$

small for Energetic Particles (EPs)

– EPs provide stabilizing force that is nearly independent of ω_ϕ

– EPs generally are <u>not</u> in mode resonance, so the effect is not energy dissipation, but rather a restoring force

[J.W. Berkery *et al.*, Phys. Plasmas **17**, 082504 (2010)]

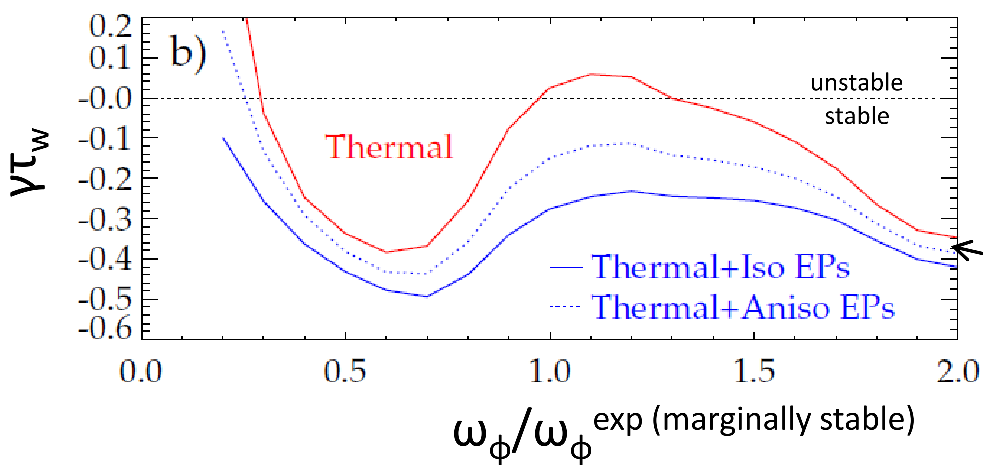

Beam ions are anisotropic

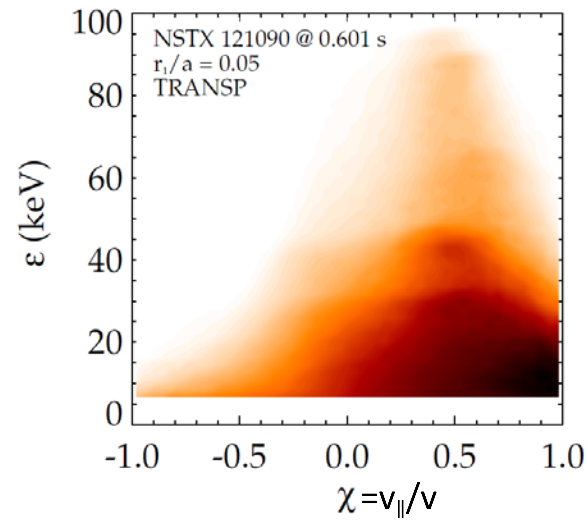

$$f(\varepsilon, \Psi, \chi) = \frac{C(\Psi)}{\varepsilon^{\frac{3}{2}} + \varepsilon_c^{\frac{3}{2}}} \frac{e^{-(\chi-\chi_0)^2/\delta\chi^2}}{\delta\chi}$$

Addition of simple anisotropy model ($\chi_0 = 0.75$, $\delta\chi = 0.25$) reduces stabilizing effect, consistent with quantitative comparison to NSTX plasmas

An NSTX experiment explored RWM stability with ω_ϕ and EP fraction, with RFA measurements, for comparison to kinetic theory

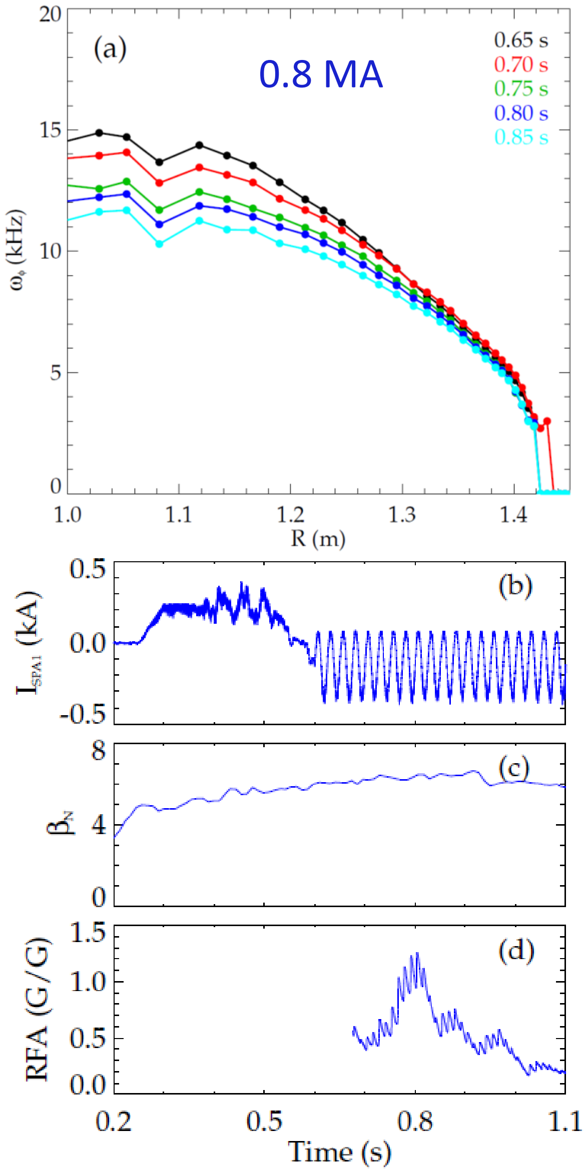

Resonant field amplification (RFA) amplitude is a measure of RWM stability.

$$RFA = \frac{B_{plasma}}{B_{applied}}$$

- ω_ϕ slowed with n=3 magnetic braking for various EP fractions (I_p, B_t scan)
  - Weak stability region at intermediate ω_ϕ shows in RFA
  - Plasma can survive it (left), or not (below).
  - Kinetic analysis with MISK was performed.
  - Many shots with long, slow, rotation decreases and many RFA periods were obtained.

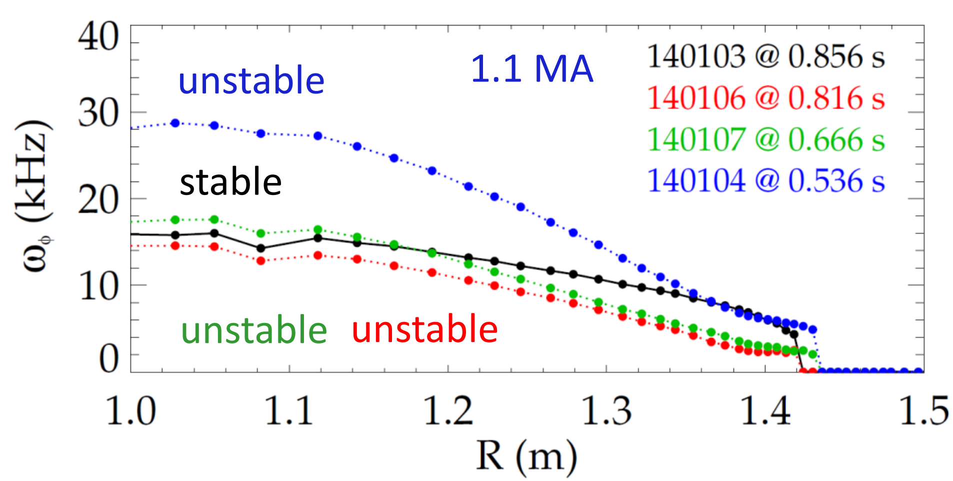

Kinetic stability calculations show reduced stability in low l_i target plasma as ω_ϕ is reduced, RWM becomes unstable

- Stability evolves

MISK code

  - MISK computation shows plasma to be stable at time of minimum l_i
  - Region of reduced stability vs. ω_ϕ found before RWM becomes unstable (l_i = 0.49)
    - Co-incident with a drop in edge density gradient – reduces kinetic stabilization

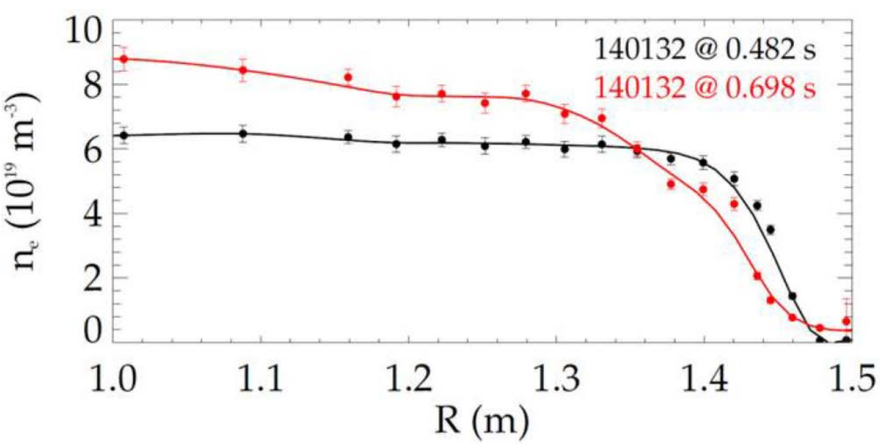

[S.A. Sabbagh *et al.*, APS Invited 2010 paper GI2.01]

RWM stability vs. ω_ϕ (contours of $\gamma\tau_w$)

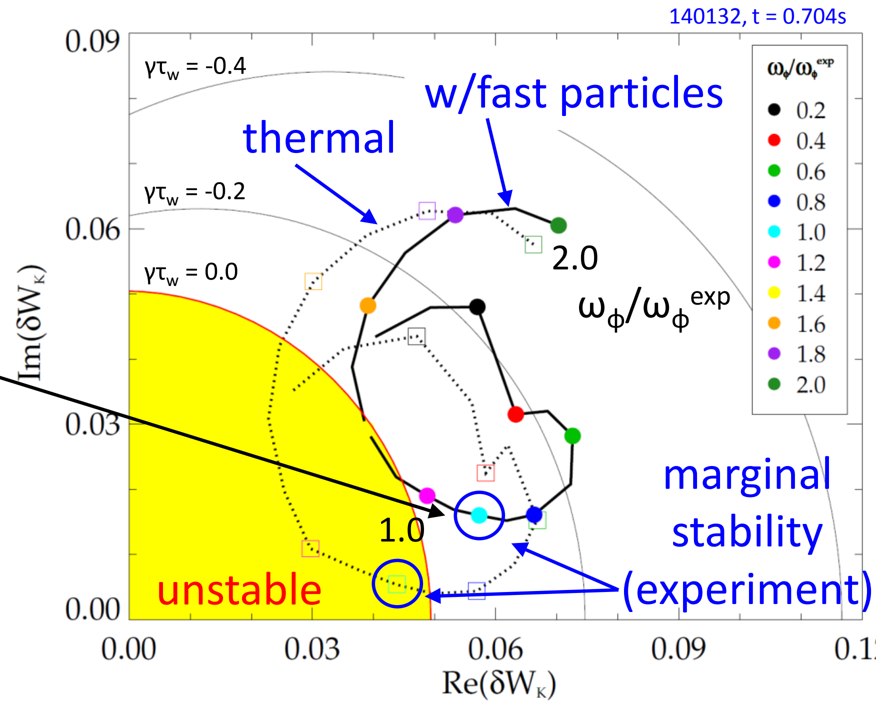

- Directly testing the RWM stability calculation at the marginal point in this NSTX experimentally unstable plasma.
- This past calculation showed close, but not full, quantitative agreement.
  - Investigating what might lead to improvement…

Kinetic stability calculations are improved by additional physics and code development

- Additional physics (EPs) improves model, but doesn't bring full agreement
  - Also improves understanding of differences between devices (see: [S. Sabbagh *et al.*, IAEA FES 2010, Paper EXS/5-5], [H. Reimerdes *et al.*, Phys. Rev. Lett. **106**, 215002 (2011)])

- Correction to ω_D from MDC-2 benchmarking further improves agreement (benchmarking investigation results later in the poster…)

Corrected ω_D

RWM stability vs. ω_ϕ (contours of $\gamma\tau_w$)

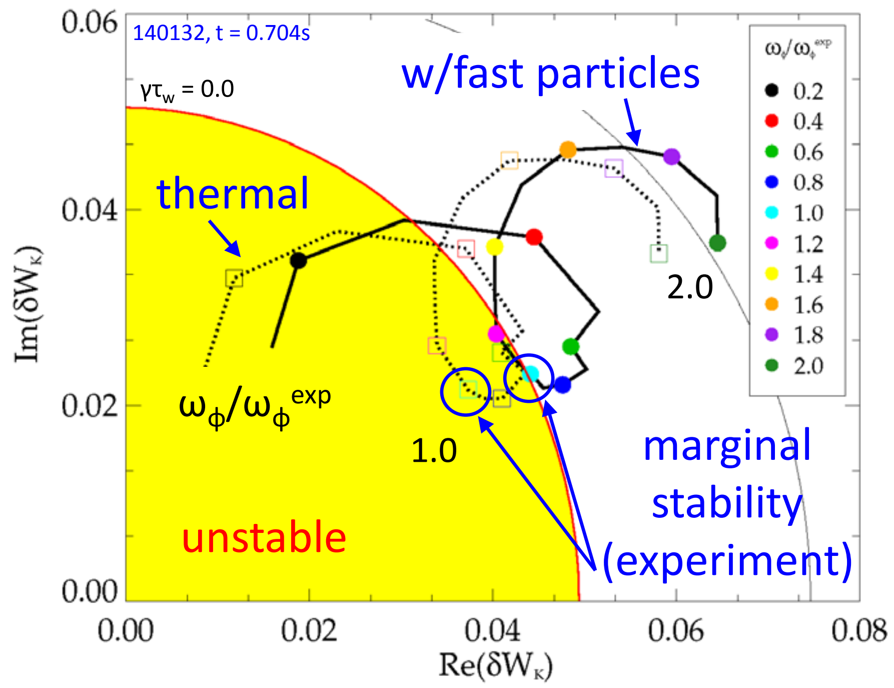

Latest NSTX experiments: Maximum RFA amplitude does not monotonically increase with increasing β_N

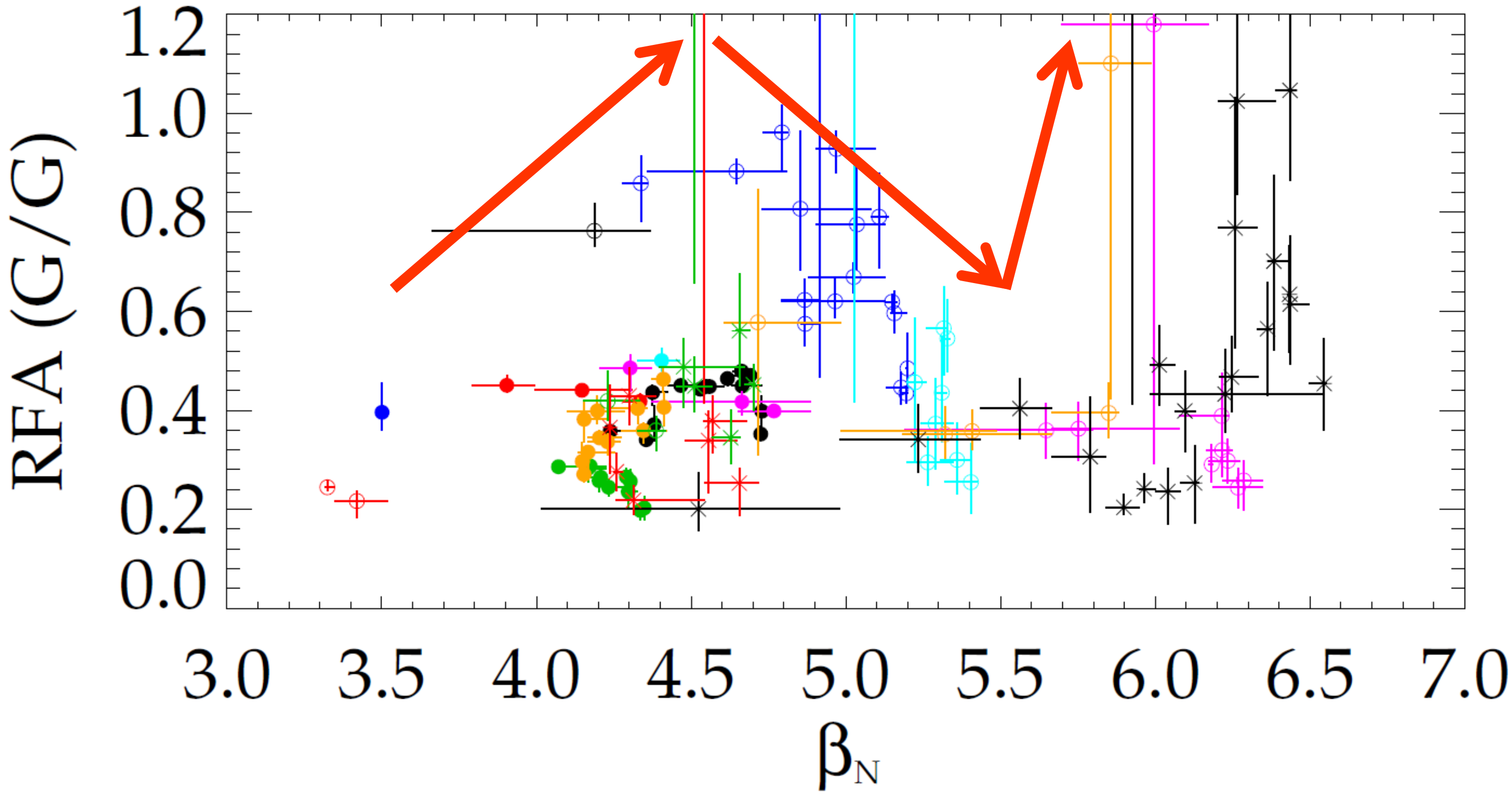

(each different symbol color/shape is from a different discharge)

- Examine resonant field amplification (RFA) amplitude to determine proximity to the marginal point
  - shows increased stability at intermediate β_N (~5.2 – 5.8).
- In other machines (DIII-D, JET) RFA increases with β_N

RFA response is greater with more peaked ω_{ϕ}, at lower β_N

- RFA response observed below n = 1 no-wall β limit
  - Common in tokamaks
- RFA increases with rotation gradient at ~ constant β_N.

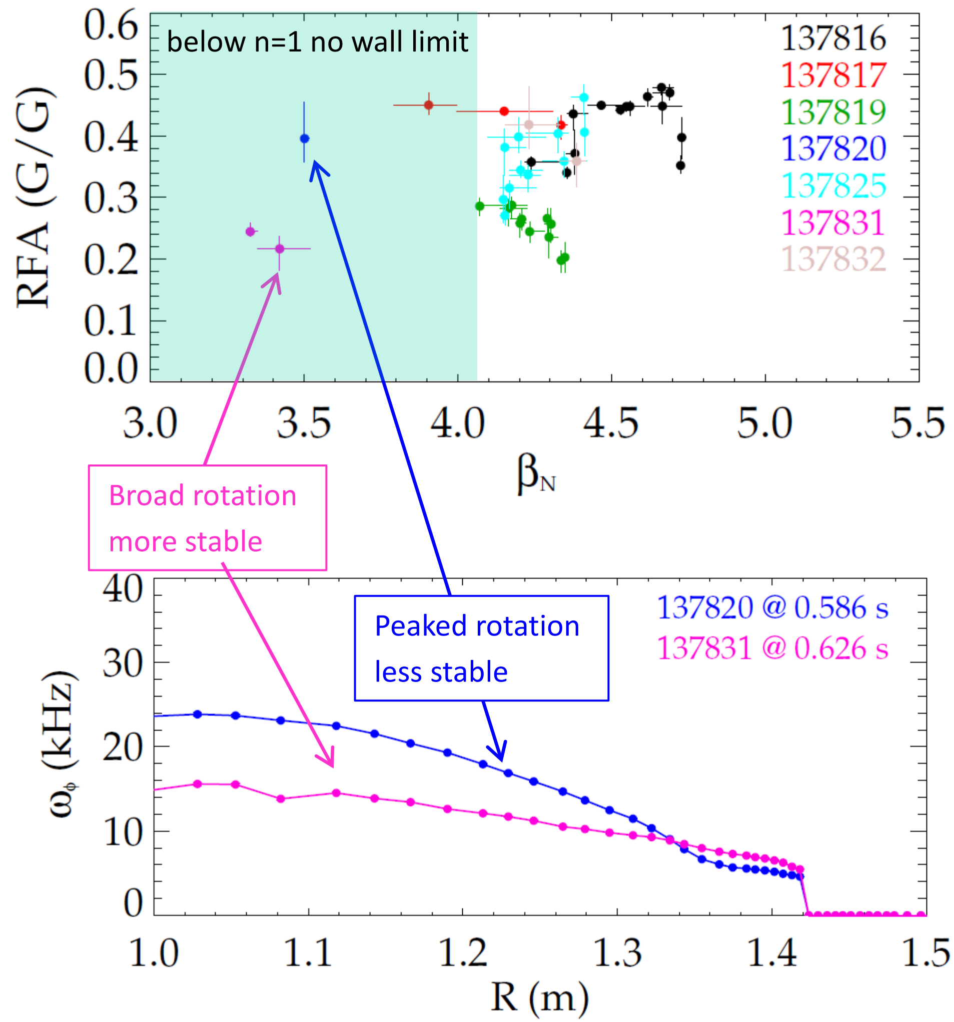

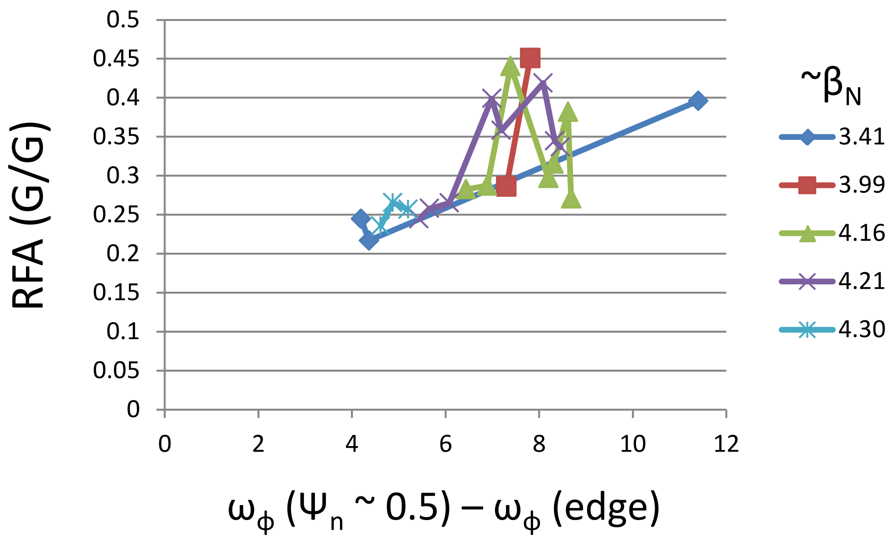

Above the no-wall limit, RWM stability dependence on ω_ϕ profiles is complex

- More specifically, RWM stability / RFA depends on energy dissipation due to kinetic resonances
  - Depends on ω_ϕ profile.
  - Sensitivity to rotation in the outer surfaces where the RWM ξ is large
- Alteration of amplitude and time history of applied n = 3 field creates ω_ϕ profile variation
- Further characterization of the approach to RWM marginal stability is underway

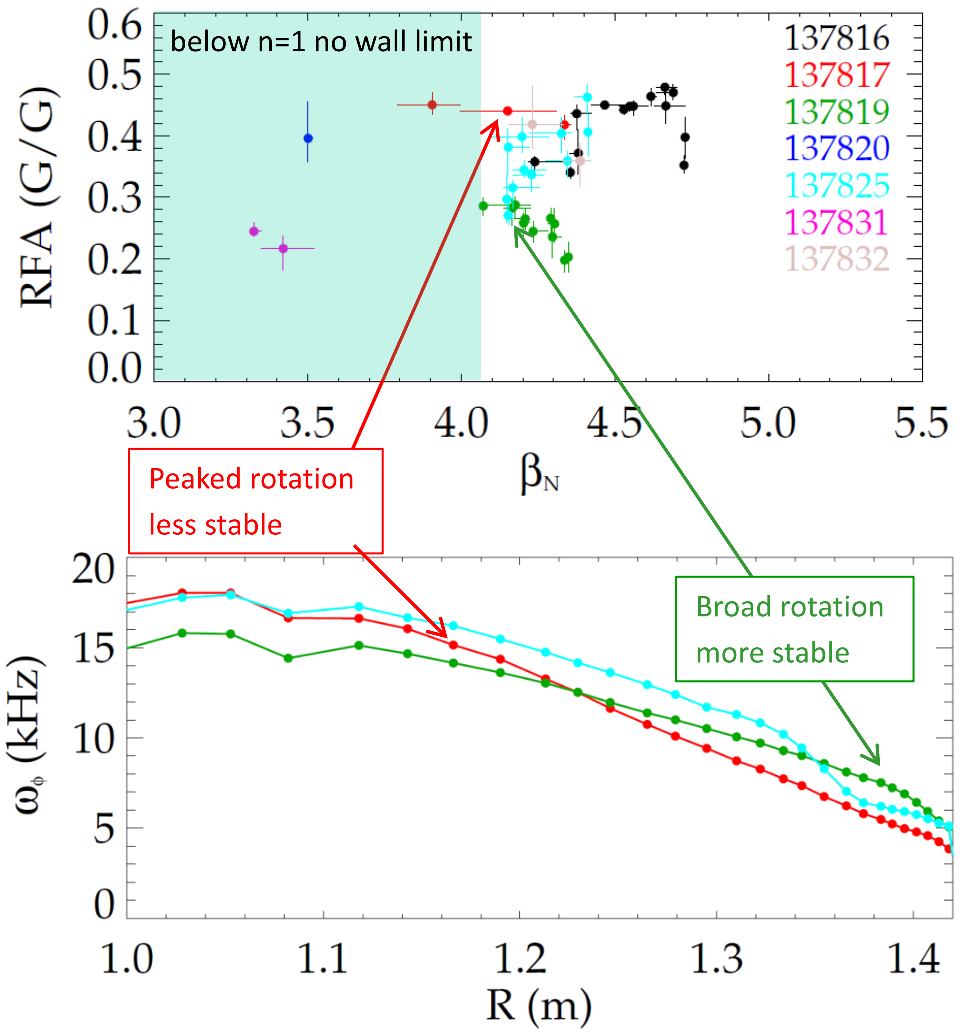

MDC-2 Benchmarking of kinetic models: overview & steps

- Codes: HAGIS, MARS-K, MISK
- Choice of equilibria for benchmarking
  - Start by using Solov'ev
    - HAGIS / MARS-K, and MISK / MARS-K benchmarked to different degrees using Solov'ev equilibria; collect/cross compare results
      - HAGIS/MARS results published [Y. Liu et al., Phys. Plasmas **15**, 112503 (2008)]
    - Simplicity may lead to unrealistic anomalies – better to use realistic cases?
  - Move on to ITER-relevant equilibria
    - Use Scenario IV, or new equilibria recently generated for WG7 task by Y. Liu (more realistic; directly applicable to ITER)
  - Need kinetic profiles as well as fluid pressure
- Approach to stability comparison – start with
  - ideal fluid quantities ($\delta W^{no\text{-}wall}$, δW^{wall}, etc.)
  - n = 1 (consider n > 1 in a future step)
  - perturbative approach on static eigenfunction input - ensure that unstable eigenfunction is consistent among codes (e.g. no-wall ideal for MISHKA)
  - no-wall / with-wall β_N limits (equilibrium β scan needed)

Spring 2011

Fall 2011

Started code comparison with simple equilibria and profile assumptions

Solov'ev case 1 (near-circular)

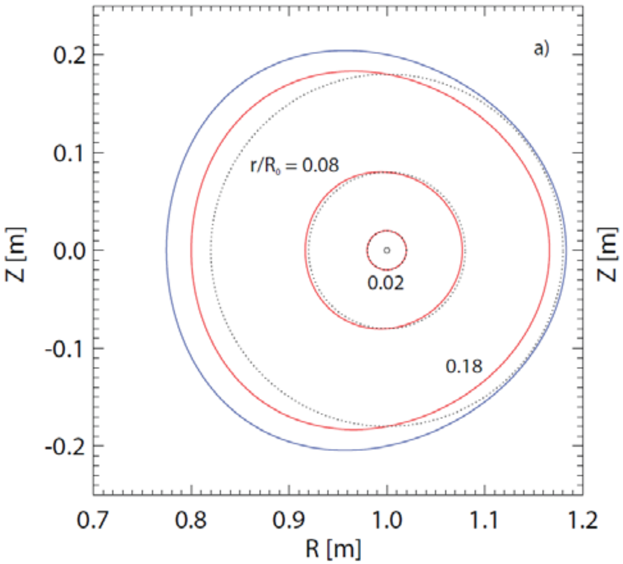

Solov'ev case 3 (shaped)

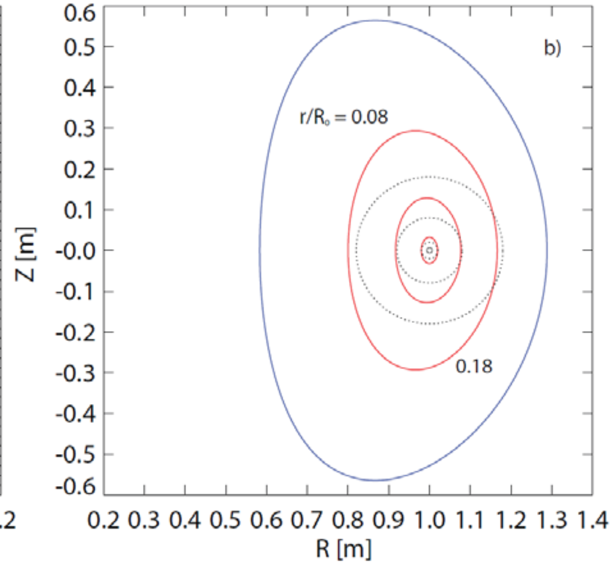

$$\mu_0 P(\psi) = -\frac{1+\kappa^2}{\kappa R_0^3 q_0}\psi, \quad F(\psi) = 1$$

$$\psi = \frac{\kappa}{2R_0^3 q_0}\left[\frac{R^2 Z^2}{\kappa^2} + \frac{1}{4}\left(R^2 - R_0^2\right)^2 - a^2 R_0^2\right]$$

$$\delta W_K \propto \int \left[\frac{\omega_{*N} + \left(\hat{\varepsilon} - \frac{3}{2}\right)\omega_{*T} + \omega_E}{\langle\omega_D\rangle + l\omega_b + \omega_E}\right]\hat{\varepsilon}^{\frac{5}{2}} e^{-\hat{\varepsilon}} d\hat{\varepsilon}$$

Simplified resonant denominator due to assumptions

- Common ground for codes (MARS / HAGIS / MISK)
  - Solov'ev equilibria
  - Codes run in perturbative mode
  - Density gradient constant
  - No energetic particles
  - ω_r, γ, $\nu_{eff} = 0$

Expanded comparison to include ITER equilibrium

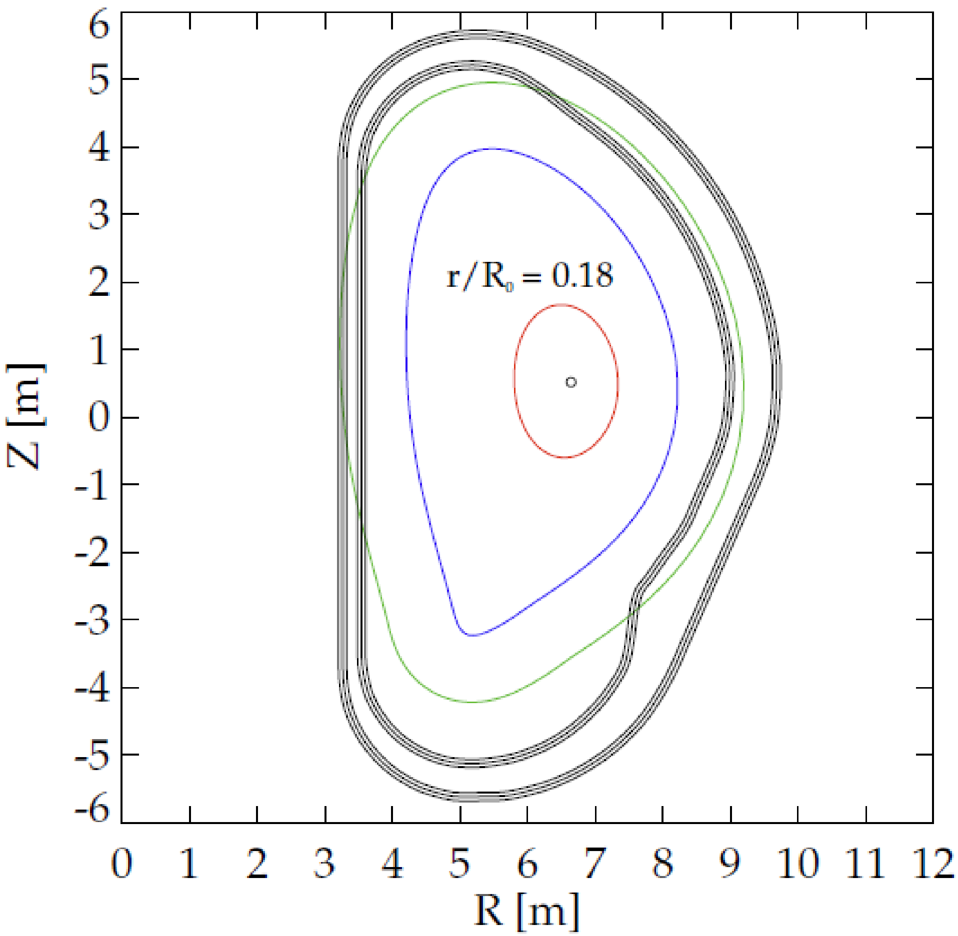

- More realistic case (ITER)
  - ITPA MHD WG7 equilibrium
    - I_p = 9 MA, β_N = 2.9 (7% above n = 1 no-wall limit)
  - Codes run in perturbative mode
  - With/without energetic particles
  - ω_r, γ, ν_{eff} = 0

$$\delta W_K \propto \int \left[\frac{\omega_{*N} + \left(\hat{\varepsilon} - \frac{3}{2}\right)\omega_{*T} + \omega_E}{\langle \omega_D \rangle + l\omega_b + \omega_E} \right] \hat{\varepsilon}^{\frac{5}{2}} e^{-\hat{\varepsilon}} d\hat{\varepsilon}$$

Note: Simplified resonant denominator due to assumptions

Shaped vs. near-circular Solov'ev cases have important q profile differences for benchmarking

Solov'ev case 1 (near-circular)

Solov'ev case 3 (shaped)

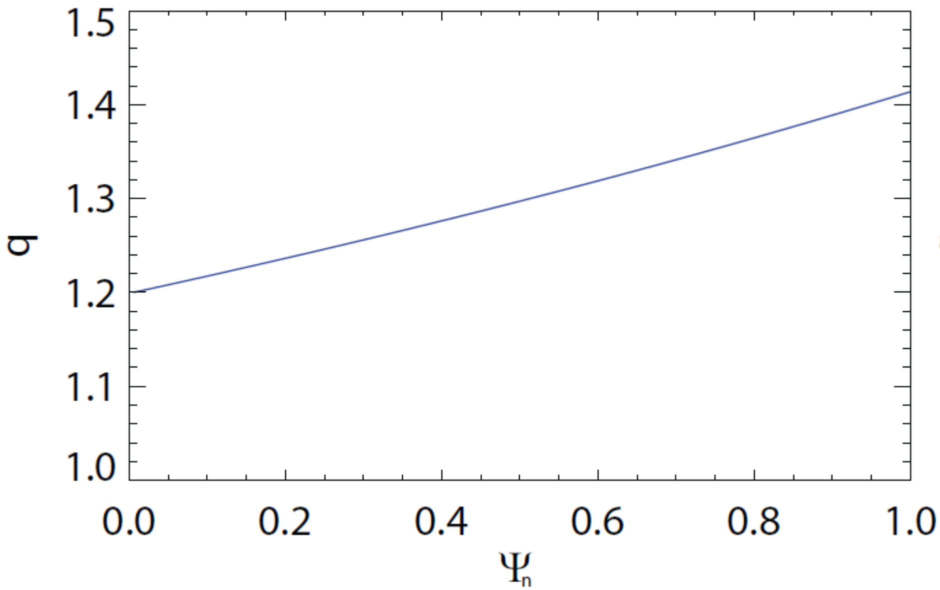

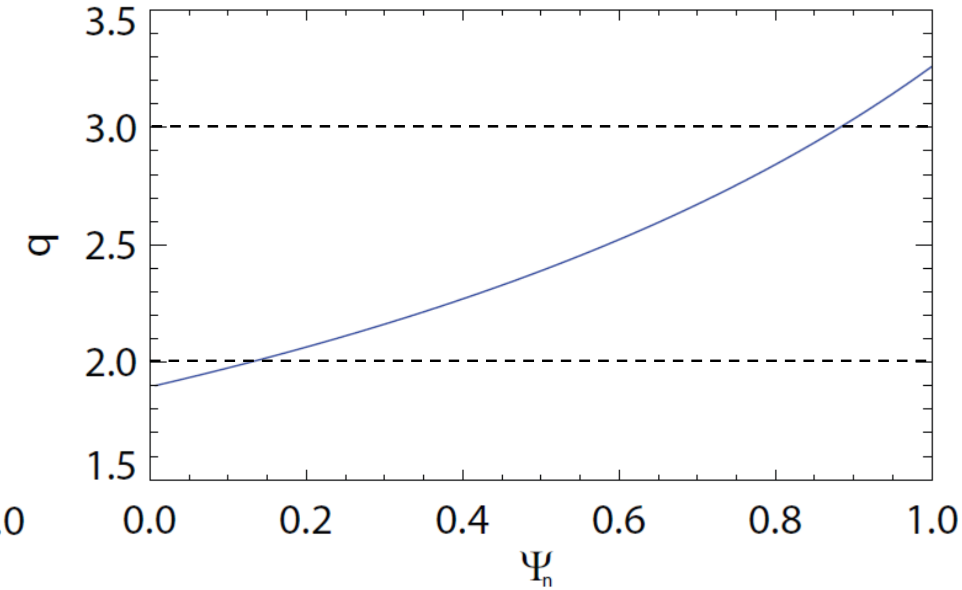

- No n = 1 rational surfaces
  - Eliminates potential differences between calculation of kinetic dissipation at rational surfaces
- Simple, key n = 1 rational surfaces
  - q = 2, 3 surfaces in the plasma
- ITER equilibrium: rev. shear, $q_0 \sim 2.2$, $q_{min} \sim 1.7$, $q_a \sim 7.1$

Differences in how MARS, MISK, HAGIS consider mode dissipation at rational surfaces is thought to be key – will be a main focus of next steps

The kinetic term can be split into two pieces that depend on the eigenfunction or the frequencies, for code comparison

Solov'ev case 1 (near-circular)

$$\delta W_K = -\frac{\sqrt{\pi}}{2}\int_0^{\Psi_a}\frac{nT}{B_0}\int_{B_0/B_{\max}}^{B_0/B_{\min}}\tau\sum_l |\langle H/\hat{\varepsilon}\rangle|^2 I_{\hat{\varepsilon}}\, d\Lambda\, d\Psi.$$

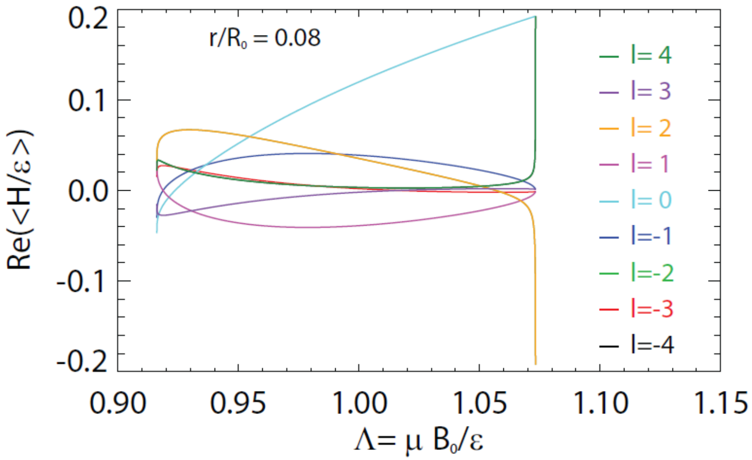

Perturbed Lagrangian

$$\langle H/\hat{\varepsilon}\rangle(\Psi,\Lambda,l) = \frac{1}{\tau}\oint\frac{1}{\sqrt{1-\frac{\Lambda B}{B_0}}}\left[\left(2-3\frac{\Lambda B}{B_0}\right)(\boldsymbol{\kappa}\cdot\boldsymbol{\xi}_\perp) - \left(\frac{\Lambda B}{B_0}\right)(\nabla\cdot\boldsymbol{\xi}_\perp)\right]e^{-il\omega_b t}d\ell.$$

- Depends mostly on the eigenfunction.

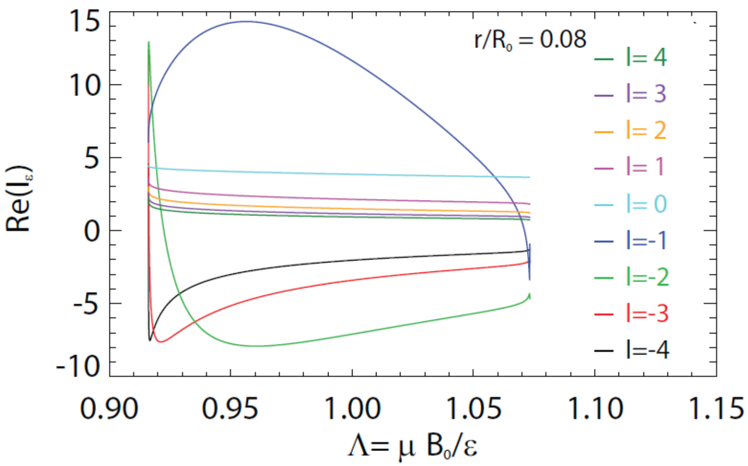

Energy integral of the frequency resonance fraction

$$I_\varepsilon(\Psi,\Lambda,l) = \int_0^\infty \frac{\omega_{*N} + \left(\hat{\varepsilon}-\frac{3}{2}\right)\omega_{*T} + \omega_E - \omega_r - i\gamma}{\omega_D + l\omega_b + \omega_E - i\nu_{\text{eff}} - \omega_r - i\gamma}\hat{\varepsilon}^{\frac{5}{2}}e^{-\hat{\varepsilon}}d\hat{\varepsilon}.$$

- Does not depend on eigenfunction, just frequency profiles

Eigenfunction benchmarking calculations were made to yield similar eigenfunctions, which are verified

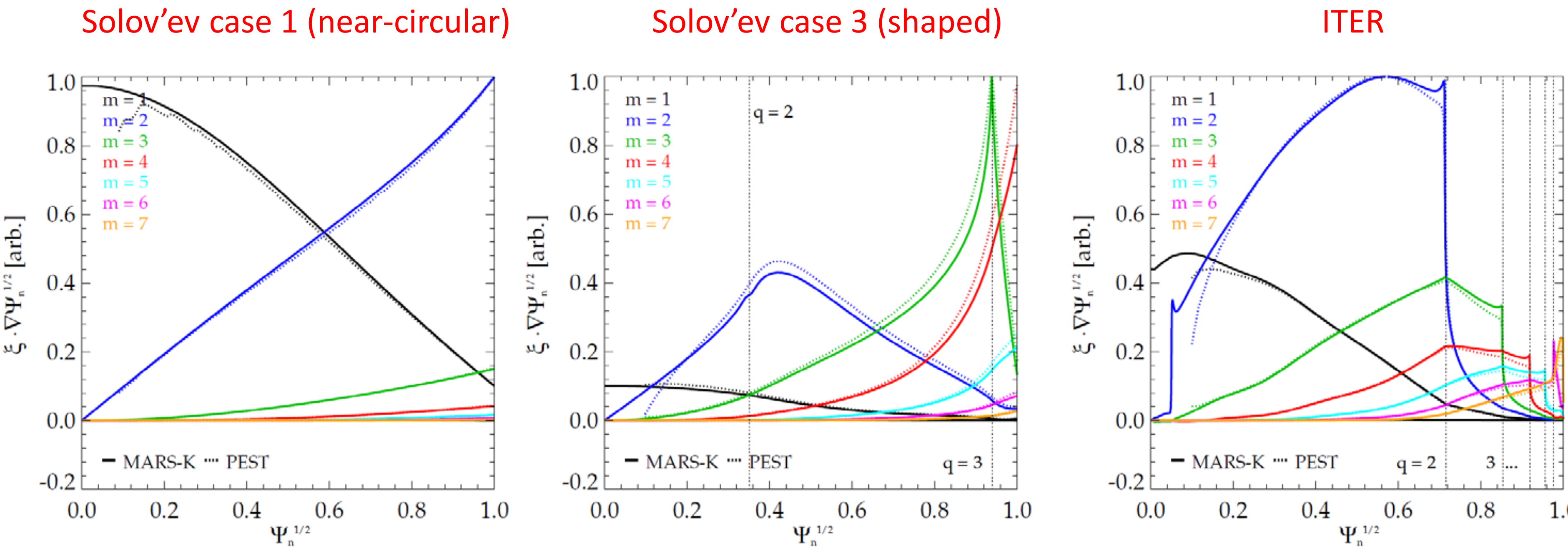

- PEST, MARS-K compared with-wall RWM
  - In PEST we use the wall position that yields marginal stability
  - PEST, MARS-K, and MISHKA compared for no-wall ideal kink
- There are some differences at rational surfaces
  - May lead to stability differences between MISK and MARS calculations

Bounce frequency vs. pitch angle compares well between codes

Solov'ev case 1 (near-circular)

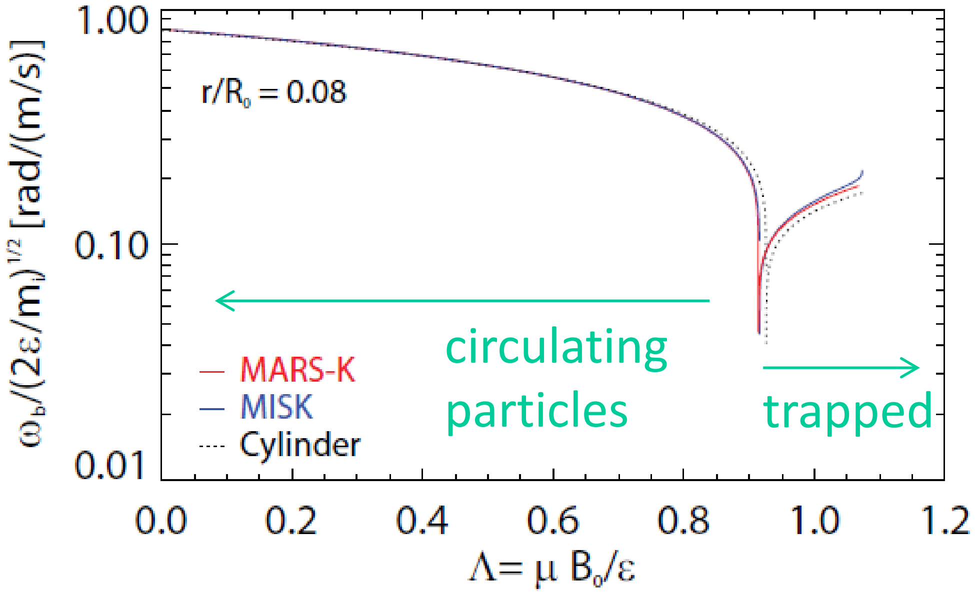

Solov'ev case 3 (shaped)

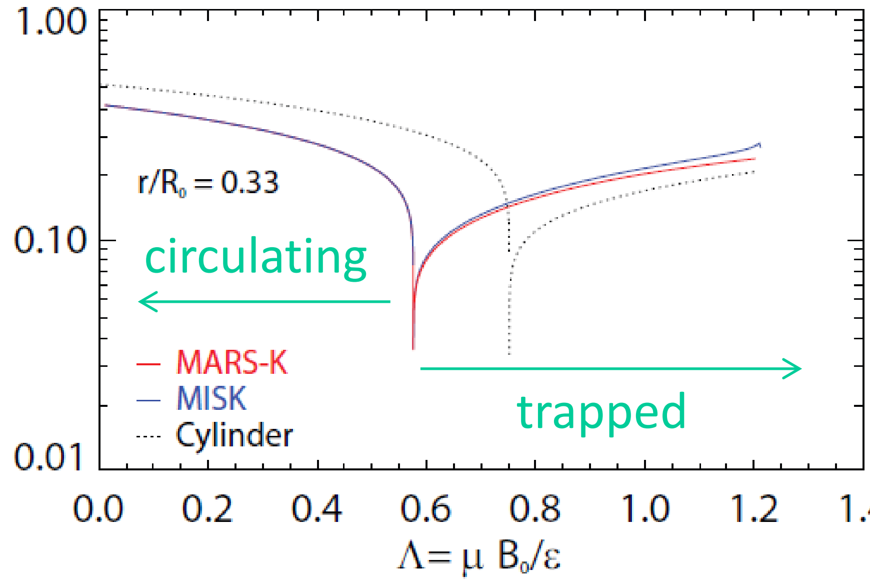

$$\frac{\omega_b}{\sqrt{2\varepsilon/m_i}} = \frac{\sqrt{2\epsilon_r \Lambda B_0}}{4qR_0}\frac{\pi}{K(k)} \quad \text{(trapped)}$$

$$k = \left[\frac{1 - \Lambda B_0 + \epsilon_r \Lambda B_0}{2\epsilon_r \Lambda B_0}\right]^{\frac{1}{2}}$$

$$\frac{\omega_b}{\sqrt{2\varepsilon/m_i}} = \frac{\sqrt{1 - \Lambda B_0 + \epsilon_r \Lambda B_0}}{2qR_0}\frac{\pi}{K(1/k)} \quad \text{(circulating)}$$

large aspect ratio approximation

here, ϵ_r is the inverse aspect ratio, s is the magnetic shear, K and E are the complete elliptic integrals of the first and second kind, and $\Lambda = \mu B_0/\varepsilon$, where μ is the magnetic moment and ε is the kinetic energy.

Bounce and precession drift frequency radial profiles agree (deeply trapped regime shown)

Bounce frequency

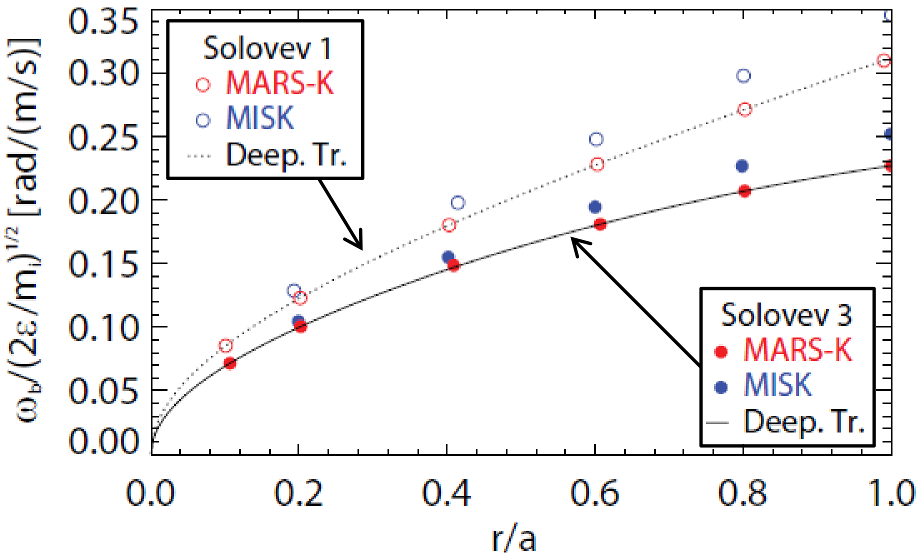

Precession drift frequency

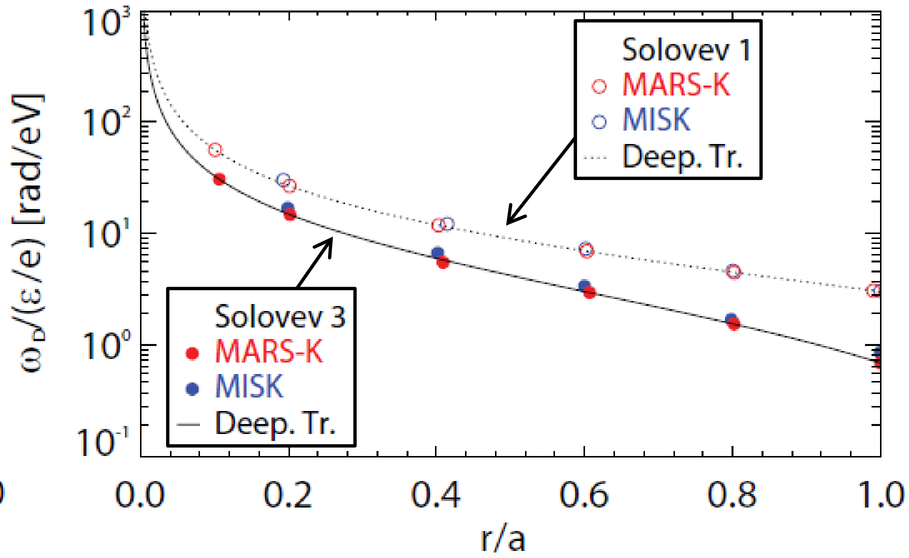

Deeply trapped limit

$$\frac{\omega_b}{\sqrt{2\varepsilon/m_i}} = \frac{1}{q_0}\left(\frac{F^2}{1+2\epsilon_r}+\frac{\kappa^2\epsilon_r^2}{q_0^2}\right)^{-1}\left[\frac{F^2\epsilon_r}{2\left(1+2\epsilon_r\right)}+\frac{\kappa^2\epsilon_r^3}{q_0^2}+\frac{\left(1-\kappa^2\right)\epsilon_r^2}{2q_0^2}\left(1+2\epsilon_r\right)\right]^{\frac{1}{2}}$$

- Good agreement across entire radial profile

Significant issue found: precession drift frequencies did not agree

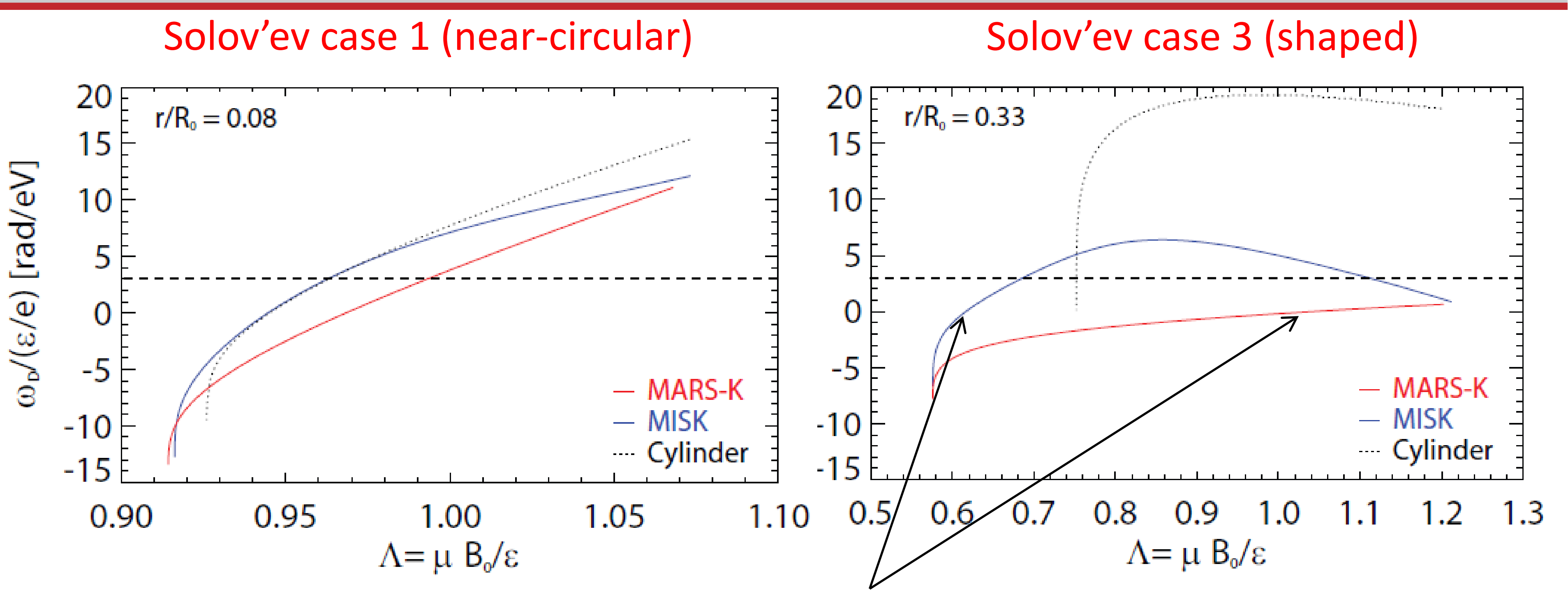

- Clear difference in drift reversal point, even in near-circular case
- Issue found and corrected: metric coefficients for non-orthogonal grid incorrect in PEST interface to MISK

large aspect ratio approximation

$$\frac{\langle \omega_D \rangle}{\varepsilon / e} = \frac{2q\Lambda}{R_0^2 B_0 \epsilon_r}\left[(2s+1)\frac{E\left(k^2\right)}{K\left(k^2\right)} + 2s\left(k^2-1\right) - \frac{1}{2}\right] \qquad k = \left[\frac{1-\Lambda+\epsilon_r\Lambda}{2\epsilon_r\Lambda}\right]^{\frac{1}{2}}$$

[Jucker et al., Phys. Plasmas 15, 112503 (2008)]

Significant issue resolved: The precession drift frequencies now agree

Solov'ev case 1 (near-circular) Solov'ev case 3 (shaped)

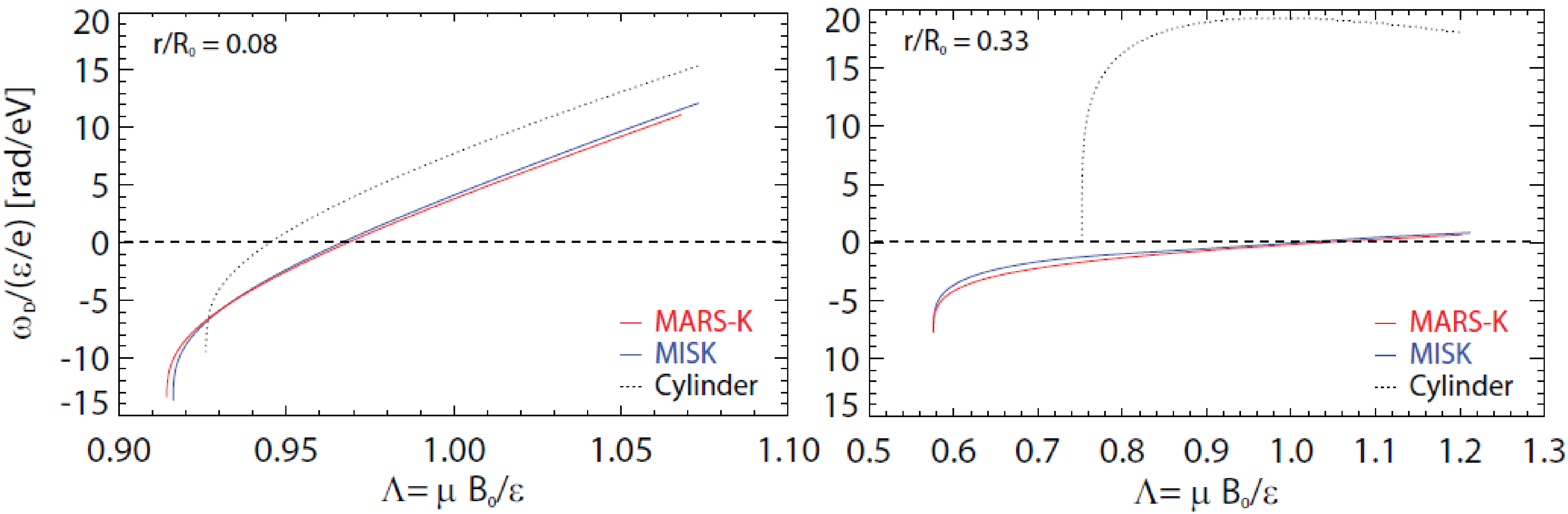

- Metric coefficients corrected in PEST interface to MISK

$$\omega_D = -\frac{1}{\tau}\int \frac{1}{v_{\|}}\mathbf{v_D}\cdot(\boldsymbol{\nabla}\phi - \hat{q}\boldsymbol{\nabla}\theta)\,d\ell - \frac{1}{\tau}\int_{\theta(t)}^{\theta(t')}\hat{q}\,d\theta.$$

if Ψ and θ are orthogonal:

$$\hat{q}\mathbf{B}\times\boldsymbol{\nabla}\theta = \frac{(\mathbf{B}_\phi\cdot\boldsymbol{\nabla}\phi)\,(\mathbf{B}_\phi\times\boldsymbol{\nabla}\theta)}{\mathbf{B}_\theta\cdot\boldsymbol{\nabla}\theta}$$

But in PEST, Ψ and θ are non-orthogonal:

$$\hat{q}\mathbf{B}\times\boldsymbol{\nabla}\theta = \frac{\mathbf{B}_\phi\cdot\boldsymbol{\nabla}\phi}{(\mathbf{B}_\phi\cdot\boldsymbol{\nabla}\theta + \mathbf{B}_\theta\cdot\boldsymbol{\nabla}\theta)}(\mathbf{B}_\phi\times\boldsymbol{\nabla}\theta + \mathbf{B}_\theta\times\boldsymbol{\nabla}\theta)$$

How does ω_D correction effect NSTX results? Mostly affects outer surfaces; characteristic change of $\gamma\tau_w$ with ω_ϕ is the same.

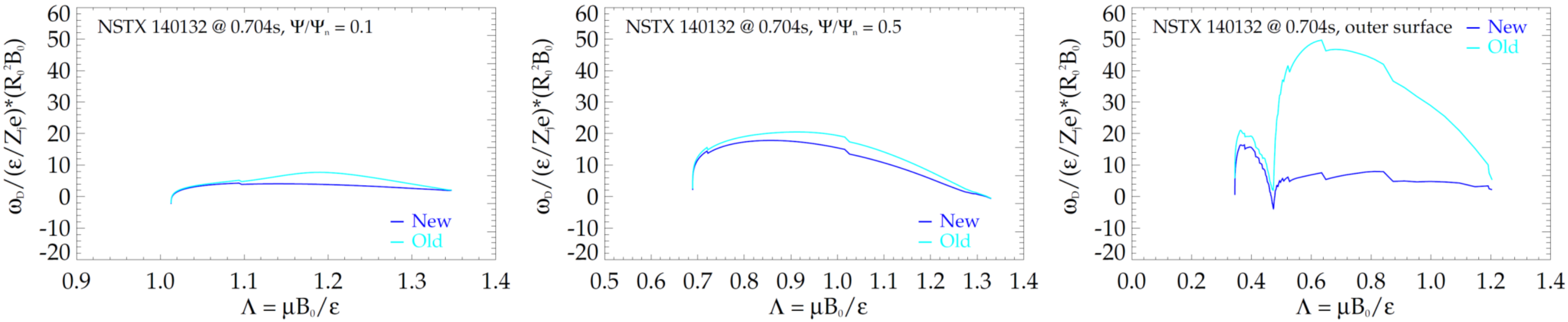

RWM stability vs. ω_ϕ (contours of $\gamma\tau_w$)

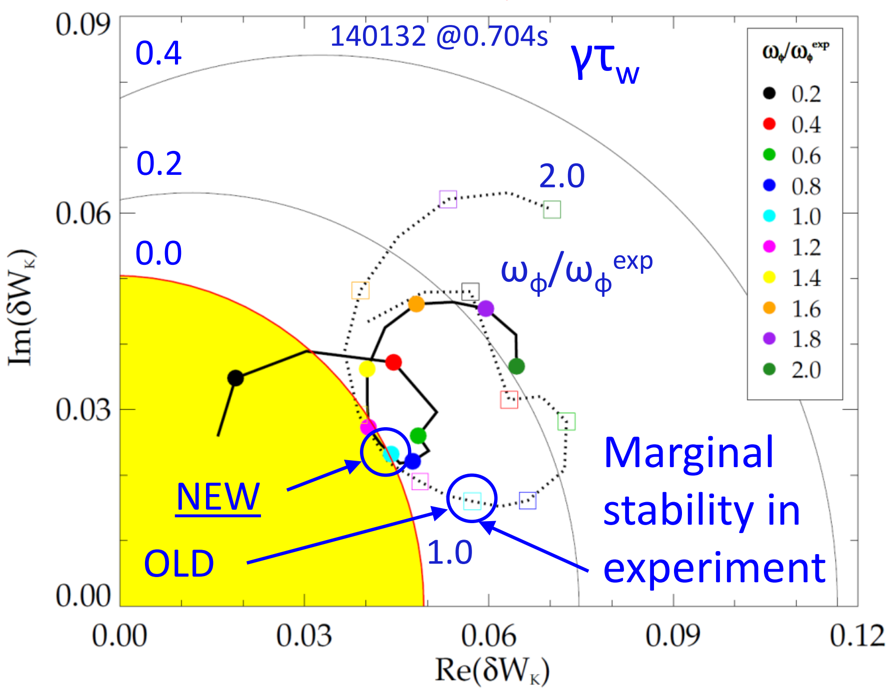

- Affects magnitude of δW_K, but not trends
- In this case, agreement with the experimental marginal point improves
  - Calculations continue to determine the effect of the correction on wider range of cases

Benchmarking process is now at the point of determining agreement in components of stability computations

Work in progress!

	r_{wall}/a	Ideal δW /(-δW_∞)	Re(δW_K) /(-δW_∞)	Im(δW_K) /(-δW_∞)	$\gamma\tau_{wall}$	$\omega\tau_{wall}$
Solov'ev 1 (MARS-K) (MISK)	1.15	1.187 1.122	0.0256 0.0243	-0.0121 0.0280	0.804 0.850	-0.0180 -0.0452
Solov'ev 3 (MARS-K) (MISK)	1.10	1.830 2.337	0.208 0.371	-0.343 0.060	0.350 0.232	-0.228 -0.027
ITER (MARS-K) (MISK)	1.50	0.682 0.677	141.5 0.665	2.286 -0.548	-0.988 0.071	0.00019 0.437

- Calculations from MISK, and MARS-K (perturbative)
  - Good agreement on ideal δW, Solov'ev 1 Re(δW_K), $\gamma\tau_{wall}$
  - Less agreement on Solov'ev 3
  - Very different ITER result

Physics Implications

Reduced collisionality (ν) is stabilizing for RWMs, but only near kinetic resonances

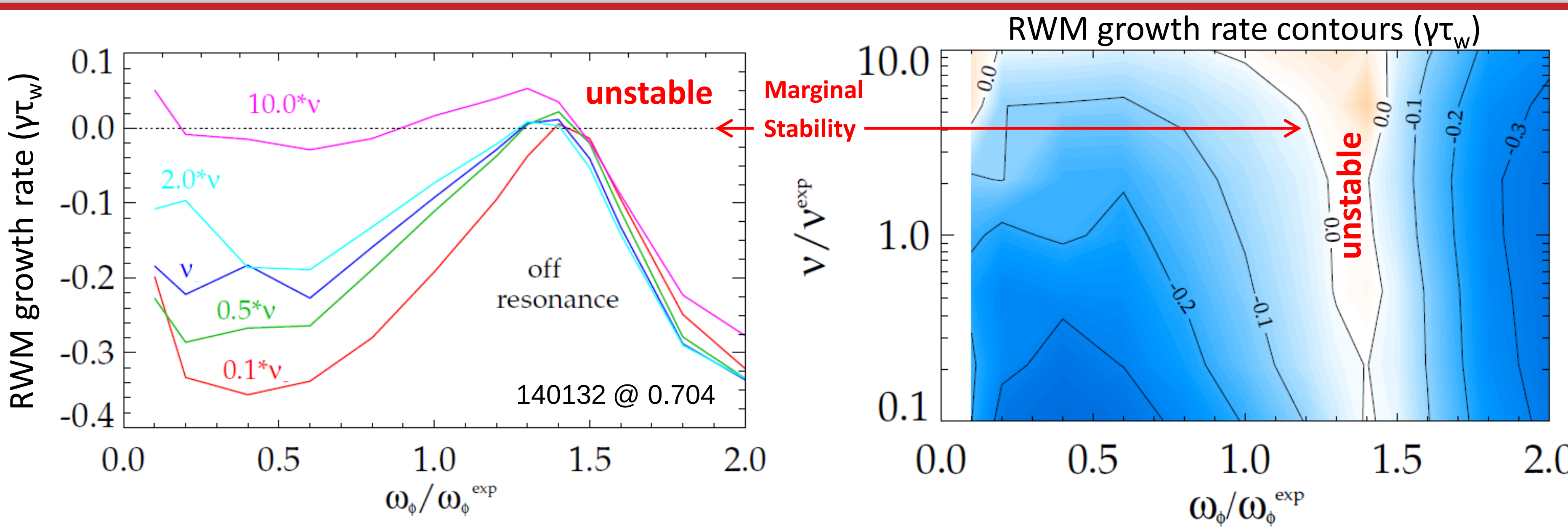

- NSTX-tested kinetic RWM stability theory: 2 competing effects at lower ν
  - Stabilizing collisional dissipation reduced (expected from early theory)
  - Stabilizing resonant kinetic effects enhanced (contrasts early RWM theory)
- Expectations in NSTX-U, tokamaks at lower ν (ITER)
  - Stronger stabilization near ω_ϕ resonances; almost no effect off-resonance
  - Plasma stability gradient with rotation increases
    - important to avoid unfavorable rotation, suppress transient RWM with active control

[J. Berkery *et al.*, Phys. Rev. Lett. **106**, 075004 (2011)]

Physics Implications

ITER requires alpha particles for RWM stability across all rotation values

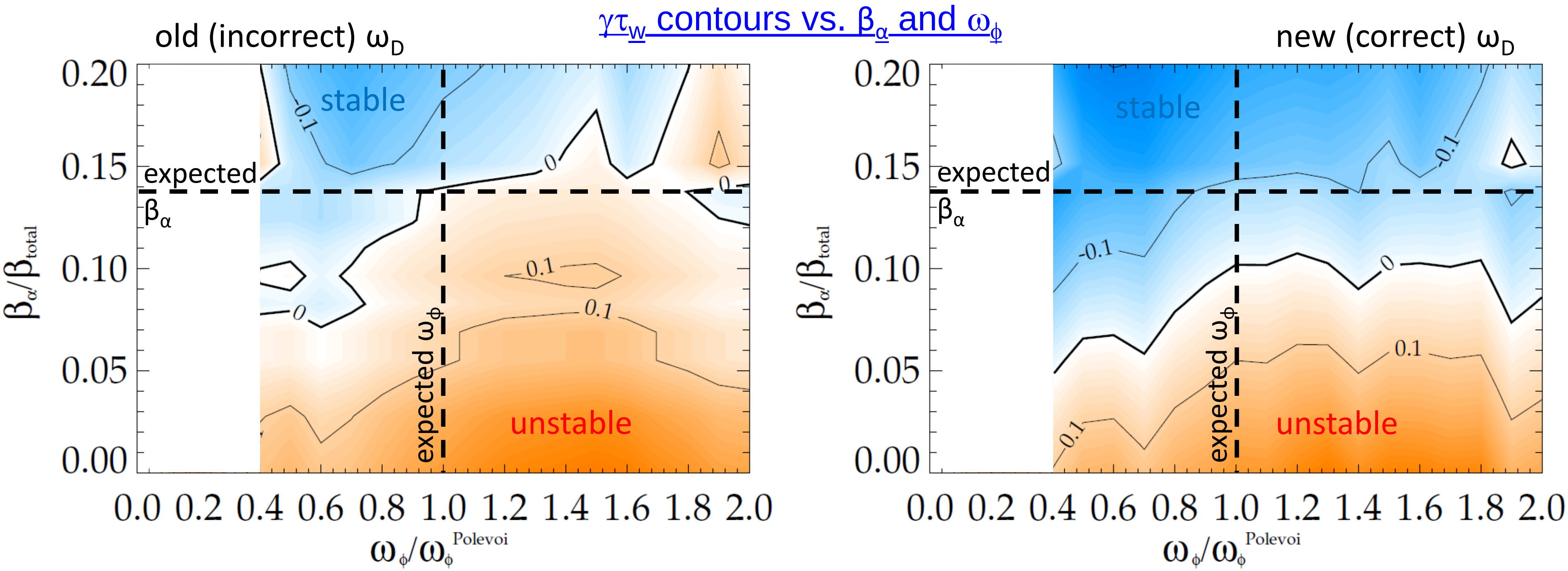

- ITER requires alpha particles for stabilization across all rotation values.
  - Quantitatively different, but generally consistent with previously analyzed case (in: [J.W. Berkery et al., Phys. Plasmas 17, 082504 (2010)])
- Correction to ω_D makes calculation more stable, but doesn't affect the general conclusions

RWM kinetic stability model is being validated by comparison to experiments and is being benchmarked with other codes

- Benchmarking:
  - Early NSTX calculations found some quantitative differences between marginal point and experiment.
  - Improved results, with additional physics (such as EPs) and code improvements, better match experiments.
  - Benchmarking exercise led to correction of ω_D calculation.
- Physics implications:
  - Energetic particles needed for quantitative agreement with NSTX; EP distribution matters.
  - Stronger stabilization near ω_ϕ resonances in low ν devices.
  - Alpha particles required for stability at all ω_ϕ in ITER.

Supported by U.S. Department of Energy Contracts: DE-FG02-99ER54524, DE-AC02-09CH11466, and DE-FG02-93ER54215

Requests for an electronic copy